

Polarization-independent two-port beam splitter grating under second Bragg incidence angle with usual duty cycle

Bo WANG

School of Physics and Optoelectronic Engineering, Guangdong University of Technology,
Guangzhou 510006, China; e-mail: wb_wsx@yahoo.com.cn

Based on the total internal reflection (TIR) under second Bragg incidence angle, polarization-independent two-port beam splitter grating etched in fused silica is described for the usual duty cycle of 0.5. There are three diffraction orders in the reflection: -2nd order, -1st order, and 0th order. The grating depth and period are optimized using the rigorous coupled-wave analysis (RCWA) in order to separate the incident wave into the -2nd and 0th orders with good uniformity and high efficiency for the TE and TM polarization wavelength of 800 nm. The diffraction properties for operation have been investigated for the incident wavelength and angle, indicating that good tolerance of incidence angle can be obtained for the designed beam splitter grating. Most importantly, the advantages of usual duty cycle of 0.5 and much shallower-etched depth will facilitate effective fabrication the reported beam splitter, which is of great significance for the practical use in numerous optical systems.

Keywords: second Bragg angle, total internal reflection, beam splitter.

1. Introduction

High-density deep-etched gratings have attracted a great deal of attention due to their novel optical properties and promising use in micro-optical elements [1–3]. And refinements in photolithography and inductively coupled plasma dry etching method make it possible to fabricate the designed and optimized grating-based diffractive optical elements for low cost mass production [4]. Such grating elements have advantages of the simple structure, high efficiency, and small feature size over conventional optical devices [5].

A series of works presented optimized high-density deep-etched gratings as the high-efficiency element [6, 7], polarizing beam splitter [8, 9], and two-port beam splitter [10, 11]. Compared with a beam splitter based on multilayer coatings, beam splitter gratings can achieve high efficiency without multiple refractions and reflections. A transmission wideband two-port beam splitter can be realized with a binary fused-silica phase grating for not only TE or TM polarization but also for both TE

and TM polarizations, where the optimized polarization-independent two-port beam splitter is with special duty cycle of 0.643 [12]. In order to improve the efficiency, a two-port beam splitter of total internal reflection (TIR) grating [13] was introduced. Such a beam splitter grating can show polarization-independent property with special duty cycle of 0.35 [14]. For easy fabrication in practice, it is desirable for a polarization-independent beam splitter with usual duty cycle of 0.5. Although a transmission polarization-independent beam splitter was designed and fabricated with optimized period of 891 nm, depth of 2.873 μm , and usual duty cycle of 0.5. The aspect ratio of grating depth to ridge width is about 6.45 [10], which may be much higher for fabrication of a transmission grating. To the best of our knowledge, no one has presented polarization-independent two-port beam splitter grating under the second Bragg incidence angle with usual duty cycle.

In this paper, we describe a polarization-independent two-port beam splitter based on TIR grating with usual duty cycle, where energies under second Bragg incidence angle are reflected in the -2nd and 0th orders. Grating period and depth are optimized using rigorous coupled-wave analysis (RCWA) [15]. The diffraction properties of wavelength range and angular bandwidth are investigated for the diffracted -2nd, -1st, and 0th orders.

2. Polarization-independent two-port beam splitter

As shown in Fig. 1, the two-port beam splitter with period d and depth h is etched in fused silica with refractive indices n_1 and $n_2 = 1$ for air, which is illuminated by a plane wave with wavelength λ under second Bragg angle of $\theta_i = \sin^{-1}(\lambda/(n_1 d))$. The polarization-independent beam splitter can separate both TE- and TM-polarized incident waves into the -2nd and 0th orders equally. The grating duty cycle f is the ratio of the ridge width to the period. Generally speaking, grating pattern can be generated by laser direct writing, electron beam, and holographic interference. For high-density deep-etched grating, small variation of duty cycle can greatly affect the diffraction

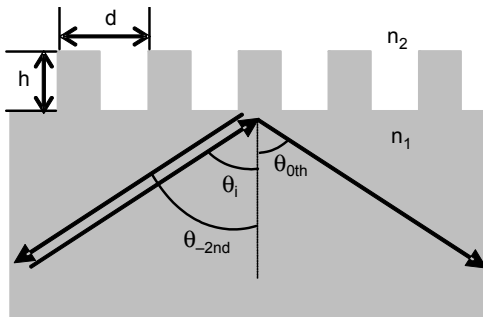


Fig. 1. Schematic of a polarization-independent two-port beam splitter based on TIR grating under second Bragg incidence angle (n_1 and n_2 refractive indices of fused silica and air, respectively, d period, h depth, θ_i incidence angle, $\theta_{0\text{th}}$ and $\theta_{-2\text{nd}}$ diffraction angles of the 0th and -2nd reflection orders in fused silica, respectively).

efficiency and property. For fabrication purposes, it is interesting for a grating with usual duty cycle of 0.5 to realize desirable optical functions.

In the design, the TIR together with the second Bragg incidence angle are taken into account. The entire incident wave can be reflected without transmission to achieve high efficiency by TIR, where the period should satisfy the inequality

$$\frac{\lambda}{n_1} < d < \frac{\lambda}{n_2} \quad (1)$$

There are three diffracted orders: -2nd order, -1st order, and 0th order. According to the grating equation, the period should vary as follows

$$\frac{\lambda}{n_1} < d < \frac{2\lambda}{n_1} \quad (2)$$

For an incident wavelength of 800 nm, the refractive index is 1.45332 for fused silica. With TIR and second Bragg incidence conditions, a range of 551–800 nm is considered in the design. The diffraction property can be widely investigated with different grating parameters. Figure 2 is the contour of the efficiency ratio between the -2nd order and 0th order versus grating period and depth for the incident wavelength of 800 nm with usual duty cycle of 0.5 under the second Bragg incidence angle. In Fig. 2, the efficiency ratio can be unity for not only TE but also TM polarization with optimized grating depth of 0.62 μm and period of 663 nm. With deviations of depth and period from the optimized results, the efficiency ratio of the -2nd to 0th order may not be equal to unity. In Fig. 2, efficiency ratios within the range of 0.8–1.25 can still be tolerated with the depth of 0.604–0.631 μm and period of

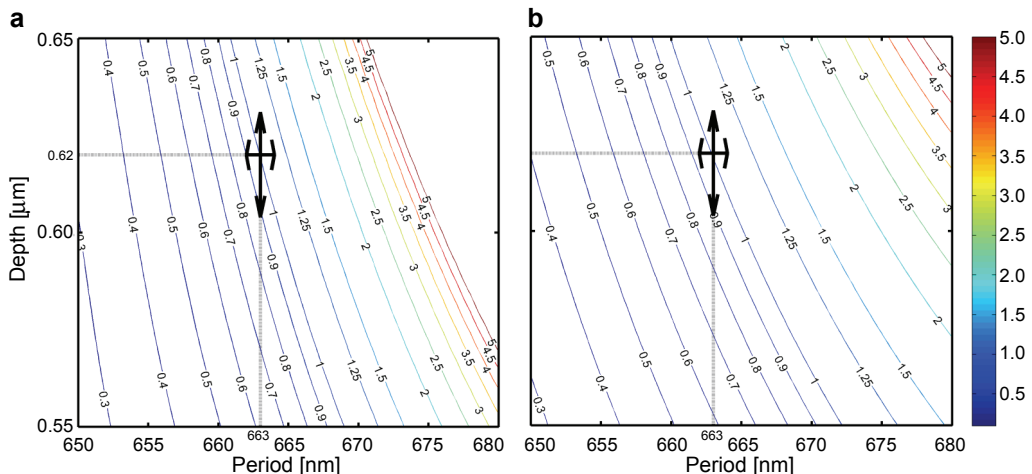


Fig. 2. The contour of the efficiency ratio between the -2nd order and 0th order versus grating period and depth for the incident wavelength of 800 nm with usual duty cycle of 0.5 under second Bragg incidence angle: TE polarization (a); TM polarization (b).

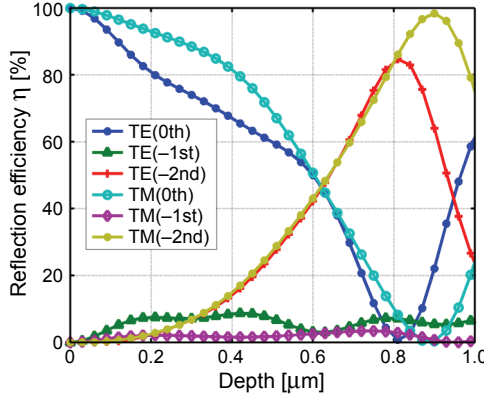


Fig. 3. The efficiency versus the grating depth under second Bragg incidence angle for the incident wavelength of 800 nm with a period of 663 nm and usual duty cycle of 0.5.

662–664 nm. Figure 3 shows the efficiency versus the grating depth under second Bragg incidence angle for the incident wavelength of 800 nm with period of 663 nm and usual duty cycle of 0.5. In Fig. 3, efficiencies of the -2nd and 0th orders for TE and TM polarizations are $\eta_{-2\text{nd}}^{\text{TE}} = 46.38\%$, $\eta_{0\text{th}}^{\text{TE}} = 46.14\%$, $\eta_{-2\text{nd}}^{\text{TM}} = 46.81\%$, and $\eta_{0\text{th}}^{\text{TM}} = 46.36\%$. This indicates that with optimized grating period and depth, the TIR grating can separate both TE and TM polarizations into different orders with uniformity under second Bragg incidence angle for the usual duty cycle of 0.5.

3. Properties for operation

Figure 4 shows the diffraction efficiency and efficiency ratio versus the incident wavelength near the 800 nm with the optimized grating parameters under second Bragg

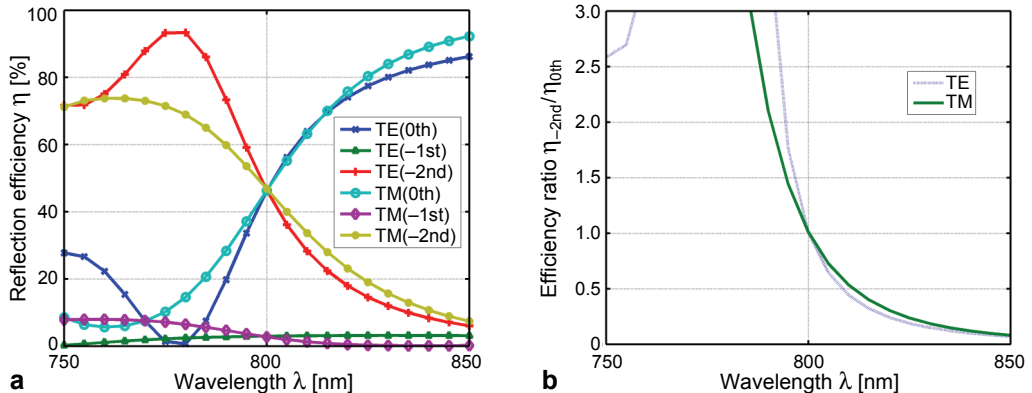


Fig. 4. Reflection efficiency (a) and efficiency ratio (b) versus the incident wavelength near the 800 nm with the optimized grating parameters under second Bragg incidence angle for the usual duty cycle of 0.5.

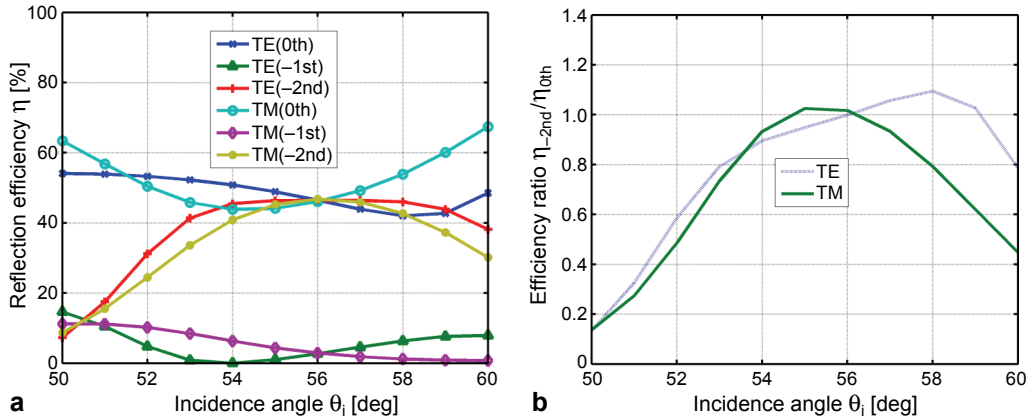


Fig. 5. Reflection efficiency (a) and efficiency ratio (b) versus the incidence angle near the second Bragg incidence angle with the optimized results and the incident wavelength of 800 nm for the usual duty cycle of 0.5.

incidence angle for the usual duty cycle of 0.5. Equal efficiency between the -2nd and 0th orders can be achieved with the wavelength of 800 nm, which will not be so uniform with deviations of wavelength. In Fig. 4, efficiency ratios of 0.8–1.25 can still be achieved within the range of 798–802 nm for both TE and TM polarizations.

Figure 5 shows the diffraction efficiency and efficiency ratio versus the incidence angle near the second Bragg incidence angle with the optimized results and the incident wavelength of 800 nm for the usual duty cycle of 0.5. It indicates that with the second Bragg incidence angle, the TIR grating can work as a polarization-independent two-port beam splitter with good uniformity. Efficiency differences between two orders may increase with incidence angle deviating from the given mounting. In Fig. 5, efficiency ratios of the -2nd to 0th orders are in the range of 0.8–1.25 with the incidence angle of 53.29°–57.95° for both TE- and TM-polarized waves. This indicates that the polarization-independent two-port beam splitter can tolerate a wide range of incidence angle.

4. Conclusions

Based on TIR under second Bragg incidence angle, a polarization-independent two-port beam splitter has been presented for the usual duty cycle of 0.5. With optimized depth of 0.62 μm and a period of 663 nm, good uniformity and high efficiency can be achieved, and the designed beam splitter can separate the incident wave into the -2nd and 0th orders for not only TE but also TM polarization. The beam splitter is designed with novel structure of TIR etched in fused silica together with the second Bragg incidence angle. Compared with reported beam splitter, the advantages of usual duty cycle and shallower-etched depth will facilitate effective fabrication.

The presented TIR fused-silica grating under second Bragg incidence angle should be useful polarization-independent beam splitter for various optical applications.

Acknowledgements – This work is supported by the National Natural Science Foundation (11147183) of China and the Foundation (LYM09065) for Distinguished Young Talents in Higher Education of Guangdong Province.

References

- [1] DELBEKE D., BAETS R., MUYS P., *Polarization-selective beam splitter based on a highly efficient simple binary diffraction grating*, Applied Optics **43**(33), 2004, pp. 6157–6165.
- [2] NÉAUPORT J., JOURNOT E., GABORIT G., BOUCHUT P., *Design, optical characterization, and operation of large transmission gratings for the laser integration line and laser megajoule facilities*, Applied Optics **44**(16), 2005, pp. 3143–3152.
- [3] CLAUSNITZER T., KÄMPFE T., KLEY E.-B., TÜNNERMANN A., TISHCHENKO A. V., PARRIAUX O., *Investigation of the polarization-dependent diffraction of deep dielectric rectangular transmission gratings illuminated in Littrow mounting*, Applied Optics **46**(6), 2007, pp. 819–826.
- [4] WANG S., ZHOU C., RU H., ZHANG Y., *Optimized condition for etching fused-silica phase gratings with inductively coupled plasma technology*, Applied Optics **44**(21), 2005, pp. 4429–4434.
- [5] PETERS D.W., BOYE R.R., WENDT J.R., KELLOGG R.A., KEMME S.A., CARTER T.R., SAMORA S., *Demonstration of polarization-independent resonant subwavelength grating filter arrays*, Optics Letters **35**(19), 2010, pp. 3201–3203.
- [6] KONTIO J.M., SIMONEN J., LEINONEN K., KUITTINEN M., NIEMI T., *Broadband infrared mirror using guided-mode resonance in a subwavelength germanium grating*, Optics Letters **35**(15), 2010, pp. 2564–2566.
- [7] KARAGODSKY V., SEDGWICK F.G., CHANG-HASNAIN C.J., *Theoretical analysis of subwavelength high contrast grating reflectors*, Optics Express **18**(16), 2010, pp. 16973–16988.
- [8] WANG B., ZHOU C., WANG S., FENG J., *Polarizing beam splitter of a deep-etched fused-silica grating*, Optics Letters **32**(10), 2007, pp. 1299–1301.
- [9] ZHENG J., ZHOU C., FENG J., WANG B., *Polarizing beam splitter of deep-etched triangular-groove fused-silica gratings*, Optics Letters **33**(14), 2008, pp. 1554–1556.
- [10] FENG J., ZHOU C., ZHENG J., CAO H., LV P., *Design and fabrication of a polarization-independent two-port beam splitter*, Applied Optics **48**(29), 2009, pp. 5636–5641.
- [11] ZHENG J., ZHOU C., WANG B., FENG J., *Beam splitting of low-contrast binary gratings under second Bragg angle incidence*, Journal of the Optical Society of America A **25**(5), 2008, pp. 1075–1083.
- [12] WANG B., ZHOU C., FENG J., RU H., ZHENG J., *Wideband two-port beam splitter of a binary fused-silica phase grating*, Applied Optics **47**(22), 2008, pp. 4004–4008.
- [13] MARCIANTE J.R., HIRSH J.I., RAGUIN D.H., PRINCE E.T., *Polarization-insensitive high-dispersion total internal reflection diffraction gratings*, Journal of the Optical Society of America A **22**(2), 2005, pp. 299–305.
- [14] WANG B., *High-efficiency two-port beam splitter of total internal reflection fused-silica grating*, Journal of Physics B: Atomic, Molecular and Optical Physics **44**(6), 2011, article 065402.
- [15] MOHARAM M.G., GRANN E.B., POMMET D.A., GAYLORD T.K., *Formulation for stable and efficient implementation of the rigorous coupled-wave analysis of binary gratings*, Journal of the Optical Society of America A **12**(5), 1995, pp. 1068–1076.

Received May 23, 2011